Cross-modulation and molecular interaction at the Cav3.3 protein between the endogenous lipids and the T-type calcium channel antagonist TTA-A2

Magali Cazade, Cindy E. Nuss, Isabelle Bidaud, J. J. Renger, V. N. Uebele, Philippe Lory, Jean Chemin

1521-0111/85/2/218–225$25.00
MOLECULAR PHARMACOLOGY

http://dx.doi.org/10.1124/mol.113.089581
Mol Pharmacol 85:218–225, February 2014

Cross-Modulation and Molecular Interaction at the $Ca_V3.3$ Protein between the Endogenous Lipids and the T-Type Calcium Channel Antagonist TTA-A2.

Magali Cazade, Cindy E. Nuss, Isabelle Bidaud, John J. Renger, Victor N. Uebele, Philippe Lory, and Jean Chemin

Institut de Génomique Fonctionnelle, Universités Montpellier 1 and 2, Centre National de la Recherche Scientifique, Unité Mixte de Recherche 5203, Institut National de la Santé et de la Recherche Médicale U661, LabEx Ion Channel Science and Therapeutics, Montpellier, France (M.C., I.B., P.L., J.C.); and Department of Neuroscience, Merck Research Laboratories, West Point, Pennsylvania (C.E.N., J.J.R., V.N.U.)

Received September 16, 2013; accepted November 8, 2013

ABSTRACT

T-type calcium channels (T/Ca_V3-channels) are implicated in various physiologic and pathophysiologic processes such as epilepsy, sleep disorders, hypertension, and cancer. T-channels are the target of endogenous signaling lipids including the endocannabinoid anandamide, the ω3-fatty acids, and the lipoamino-acids. However, the precise molecular mechanism by which these molecules inhibit T-current is unknown. In this study, we provided a detailed electrophysiologic and pharmacologic analysis indicating that the effects of the major *N*-acyl derivatives on the $Ca_V3.3$ current share many similarities with those of TTA-A2 [(*R*)-2-(4-cyclopropylphenyl)-*N*-(1-(5-(2,2,2-trifluoroethoxy)pyridin-2-yl)ethyl)acetamide], a synthetic T-channel inhibitor. Using radioactive binding assays with the TTA-A2 derivative [^{3}H]TTA-A1 [(*R*)-2-(4-(*tert*-butyl)phenyl)-*N*-(1-(5-methoxypyridin-2-yl)ethyl)acetamide], we demonstrated that polyunsaturated lipids, which inhibit the $Ca_V3.3$ current, as *N*AGly (*N*-arachidonoyl glycine), *N*ASer (*N*-arachidonoyl-L-serine), anandamide, *N*ADA (*N*-arachidonoyl dopamine), *N*ATau (*N*-arachidonoyl taurine), and *N*A-5HT (*N*-arachidonoyl serotonin), all displaced [^{3}H]TTA-A1 binding to membranes prepared from cells expressing $Ca_V3.3$, with K_i in a micromolar or submicromolar range. In contrast, lipids with a saturated alkyl chain, as *N*-arachidoyl glycine and *N*-arachidoyl ethanolamine, which did not inhibit the $Ca_V3.3$ current, had no effect on [^{3}H]TTA-A1 binding. Accordingly, bio-active lipids occluded TTA-A2 effect on $Ca_V3.3$ current. In addition, TTA-Q4 [(*S*)-4-(6-chloro-4-cyclopropyl-3-(2,2-difluoroethyl)-2-oxo-1,2,3,4-tetrahydroquinazolin-4-yl)benzonitrile], a positive allosteric modulator of [^{3}H]TTA-A1 binding and TTA-A2 functional inhibition, acted in a synergistic manner to increase lipid-induced inhibition of the $Ca_V3.3$ current. Overall, our results demonstrate a common molecular mechanism for the synthetic T-channel inhibitors and the endogenous lipids, and indicate that TTA-A2 and TTA-Q4 could be important pharmacologic tools to dissect the involvement of T-current in the physiologic effects of endogenous lipids.

Introduction

Low-voltage-activated (T-type/Ca_V3) calcium channels are a subclass of voltage-dependent calcium channels allowing calcium entry near the resting potential of most cells (Perez-Reyes, 2003). T-channels are implicated in many physiologic processes as diverse as neuronal firing (Perez-Reyes, 2003; Cain and Snutch, 2010), slow wave sleep (Lee and Shin, 2007), hormone secretion (Weiss and Zamponi, 2013), the cell cycle (Lory et al., 2006), heart rhythm (Ono and Iijima, 2010), and vasodilatation (Kuo et al., 2011). They emerge as important pharmacologic targets in several diseases such as epilepsy, insomnia, neuropathic pain, cancer, and hypertension (McGivern, 2006; Todorovic and Jevtovic-Todorovic, 2013).

Various synthetic T-channel blockers have been described in the past few years (McGivern, 2006; Lory and Chemin, 2007; Giordanetto et al., 2011), including TTA-A2 [(*R*)-2-(4-cyclopropylphenyl)-*N*-(1-(5-(2,2,2-trifluoroethoxy)pyridin-2-yl)ethyl)acetamide], a potent and specific inhibitor of T-current (Uebele et al., 2009a,b; Kraus et al., 2010; Reger et al., 2011). In vivo studies have demonstrated that TTA-A2 reduces

This work was supported by the French Ministry of Research Agence Nationale pour la Recherche [Grant ANR-09-MNPS-035].
dx.doi.org/10.1124/mol.113.089581.

ABBREVIATIONS: BAPTA, 1,2-bis(o-aminophenoxy)ethane-*N*,*N*,*N*′,*N*′-tetraacetic acid; CP-55940, (1*R*,3*R*,4*R*)-3-[2-hydroxy-4-(1,1-dimethylheptyl)phenyl]-4-(3-hydroxypropyl)cyclohexan-1-ol; FAAH, fatty acid amide hydrolase; 18:2 Gly, *N*-linoleoyl glycine; 20:0 Gly, *N*-arachidoyl glycine; 22:6 Gly, *N*-docosahexaenoyl glycine; HEK, human embryonic kidney cells; HP, holding potential; *N*AAla, *N*-arachidonoyl alanine; *N*ADA, *N*-arachidonoyl dopamine; *N*AEA, *N*-arachidonoyl ethanolamine (anandamide); *N*AGABA, *N*-arachidonoyl-gaba-butyric acid; *N*AGABA-OH, *N*-arachidonoyl-3-OH-gaba-butyric acid; *N*AGly, *N*-arachidonoyl glycine; *N*A-5HT, *N*-arachidonoyl serotonin; *N*ASer, *N*-arachidonoyl-L-serine; *N*ATau, *N*-arachidonoyl taurine; PMSF, phenylmethylsulfonyl fluoride; T-channel, T-type calcium channel; TTA-A1, (*R*)-2-(4-(*tert*-butyl)phenyl)-*N*-(1-(5-methoxypyridin-2-yl)ethyl)acetamide; TTA-A2, (*R*)-2-(4-cyclopropylphenyl)-*N*-(1-(5-(2,2,2-trifluoroethoxy)pyridin-2-yl)ethyl)acetamide; TTA-Q4, (*S*)-4-(6-chloro-4-cyclopropyl-3-(2,2-difluoroethyl)-2-oxo-1,2,3,4-tetrahydroquinazolin-4-yl)benzonitrile.

absence epilepsy seizures (Uebele et al., 2009b; Reger et al., 2011), pain perception (Francois et al., 2013), nicotine self-administration (Uslaner et al., 2010), and weight gain (Uebele et al., 2009a), and it ameliorates the sleep quality (Uebele et al., 2009a; Kraus et al., 2010; Reger et al., 2011) and displays antipsychotic properties (Uslaner et al., 2012).

T-channels are also inhibited by several endogenous signaling lipids. These molecules include arachidonic acid, ω3-fatty acids, endocannabinoids (as anandamide), lipo-amino-acids and lipo-neurotransmitters (Zhang et al., 2000; Chemin et al., 2001, 2007; Talavera et al., 2004; Danthi et al., 2005; Barbara et al., 2009; Ross et al., 2009; Gilmore et al., 2012). These lipids are implicated in multiple physiologic functions and more specifically in pain perception (Bradshaw and Walker, 2005; Burstein, 2008; Basbaum et al., 2009), sleep and epilepsy (Chen and Bazan, 2005), and heart rhythm and vasodilatation (Roman, 2002; Leaf et al., 2003).

Lipid-mediated inhibition of the T-current occurs in excised cell-free membrane patches consistent with the direct effect of lipids on T-channels or via perturbation of their near membrane environment (Chemin et al., 2001, 2007; Talavera et al., 2004; Barbara et al., 2009). In this context, it is interesting to note that a radiolabeled derivative of TTA-A2, [^{3}H]TTA-A1 [(*R*)-2-(4-(*tert*-butyl)phenyl)-*N*-(1-(5-methoxypyridin-2-yl)ethyl)acetamide], was shown to bind membranes from cells expressing $Ca_v3.3$ with a K_d of 1.8 nM (Uebele et al., 2009b). Moreover a structurally distinct antagonist, TTA-Q4 [(*S*)-4-(6-chloro-4-cyclopropyl-3-(2,2-difluoroethyl)-2-oxo-1,2,3,4-tetrahydroquinazolin-4-yl)benzonitrile], increased both [^{3}H]TTA-A1 binding and TTA-A2-induced inhibition of the $Ca_v3.3$ current by acting on a distinct molecular site of the $Ca_v3.3$ protein (Uebele et al., 2009b). In this study, we used these new pharmacologic tools to explore whether bioactive lipids and TTA-A2 share similar mechanisms and molecular determinants at the $Ca_v3.3$ protein.

Materials and Methods

Cell Culture and Transfection Protocols. We cultivated tsA-201 (SV40 temperature-sensitive T antigen transformed) cells and a human embryonic kidney (HEK) 293 cell line stably expressing $Ca_v3.3$ [a generous gift from Dr. Perez-Reyes (Xie et al., 2007)] in Dulbecco's modified Eagle's medium supplemented with GlutaMax and 10% fetal bovine serum (Invitrogen/Life Technologies, Carlsbad, CA). The tsA-201 cell transfection was performed using jet-PEI (QBiogene, Illkirch, France) with a DNA mix containing 0.5% of a green fluorescent protein plasmid and 99.5% of either of the plasmid constructs that code for human $Ca_v3.1a$, $Ca_v3.2$, and $Ca_v3.3$. Two days after transfection, cells were dissociated with Versene (Invitrogen) and plated at a density of $\sim 35 \times 10^3$ cells per 35-mm Petri dish for electrophysiologic recordings.

Electrophysiologic Recordings. Macroscopic currents were recorded in the whole-cell configuration using an Axopatch 200B amplifier (Molecular Devices, Sunnyvale, CA). The extracellular solution contained the following (in mM): 135 NaCl, 20 TEACl, 2 $CaCl_2$, 1 $MgCl_2$, and 10 HEPES (pH adjusted to 7.25 with KOH ~330 mOsm). Borosilicate glass pipettes have a typical resistance of 1.5–2.5 MΩ when filled with an internal solution containing the following (in mM): 140 CsCl, 10 EGTA, 10 HEPES, 3 Mg-ATP, 0.6 GTPNa, and 3 $CaCl_2$ (pH adjusted to 7.25 with KOH ~315 mOsm). In a subset of experiments, EGTA was substituted with 10 mM BAPTA [1,2-bis(o-aminophenoxy)ethane-*N*,*N*,*N*′,*N*′-tetraacetic acid]. Recordings were performed at room temperature and were filtered at 2–5 kHz. Data were analyzed using pCLAMP9 (Molecular Devices) and GraphPad Prism (GraphPad Software, Inc., San Diego, CA). Drugs were applied by a gravity-driven homemade perfusion device, and the control experiments were performed using the solvent alone. Results are presented as the mean ± S.E.M., and n is the number of cells used. Student's t test was used to compare the different values, and $P < 0.05$ was considered statistically significant.

Binding Experiments. Membranes were prepared from the HEK-293 cells stably expressing $Ca_v3.3$ (Uebele et al., 2009b). The protein concentration was determined using a protein assay (Bio-Rad Laboratories, Hercules, CA). Binding assays were performed at room temperature for 3 hours with 8 μg protein, 1 nM [^{3}H]TTA-A1, and increasing concentrations of lipids (ranging from 1 nM to 40 μM) in 1 ml final volume in Unifilter-96 GF/C plates (Packard, Meriden, CT) coated with 0.3% ethylene imine polymer solution (Sigma-Aldrich, St. Louis, MO). The assay and wash buffer contained 20 mM HEPES, 125 mM NaCl, and 5 mM KCl.

After incubation, the reactions were aspirated and washed with 4°C buffer using a 96-well Filtermate Harvester (PerkinElmer Life and Analytic Sciences, Shelton, CT). The plates were dried before the addition of Microscint-20 (PerkinElmer), and the remaining radioactivity was quantified on a PerkinElmer NXT HTS Top Count. Total and nonspecific binding were determined in the absence and the presence of 100 nM of TTA-A2, respectively.

Data were collected in triplicate. The inhibition constants K_i were calculated with GraphPad Prism using the following equation:

$$K_i = \frac{IC_{50}}{\left(1 + \left([[^3\text{H}]\text{TTA-A1}]/K_d\right)\right)},$$

where IC_{50} was the half maximal inhibitory concentration, [^{3}H]TTA-A1 was 1 nM, and K_d was 1.8 nM, as previously described elsewhere (Uebele et al., 2009b).

Chemical Reagents. [^{3}H]TTA-A1 (56–65 mCi/mmol), TTA-A2, and TTA-Q4 were synthesized at Merck (West Point, PA), as previously described elsewhere (Uebele et al., 2009b), dissolved in dimethylsulfoxide at 10 mM, aliquoted, and kept at −20°C. Lipids were obtained from Cayman Chemicals (Ann Arbor, MI) and were dissolved in ethanol purged with argon at a concentration of 10 mM. *N*A-5HT (*N*-arachidonoyl serotonin) and *N*ADA (*N*-arachidonoyl dopamine) were also obtained from Tocris Bioscience (Bristol, UK) and Enzo Life Sciences (Farmingdale, NY), and the results were similar using lipids from different suppliers. Stock lipid solutions were briefly sonicated, aliquoted, sealed under argon, and kept at −80°C. These aliquots were dissolved daily in the extracellular solution. Control experiments were performed using the solvent alone.

Results

Inhibition of $Ca_v3.3$ Currents by Polyunsaturated Amino Acids. We have characterized the effects of lipo-amino-acids on the $Ca_v3.3$ current because among lipids inhibiting T-currents, only this class showed a higher T-type specificity with no effect on cannabinoid receptors and transient receptor potential vanilloid-1 (Huang et al., 2001; Bradshaw and Walker, 2005; Barbara et al., 2009). We found that the $Ca_v3.3$ current was strongly inhibited by 3 μM *N*-docosahexaenoyl glycine (22:6 Gly; chain length 22 carbons, 6 double bonds) at a holding potential (HP) of −75 mV (Fig. 1A) but not at HP −110 mV (Fig. 1B). The inhibition occurred in the minute range and was relieved by application of 3 mg/ml of bovine serum albumin (Barbara et al., 2009; Gilmore et al., 2012) (Fig. 1C). The extent of inhibition increased gradually with the number of double bonds in *N*-acyl glycine (Fig. 1E). Saturated *N*-arachidoyl glycine (20:0 Gly) produced weak inhibition (~13%, $n = 5$; Fig. 1, D and E); *N*-linoleoyl glycine

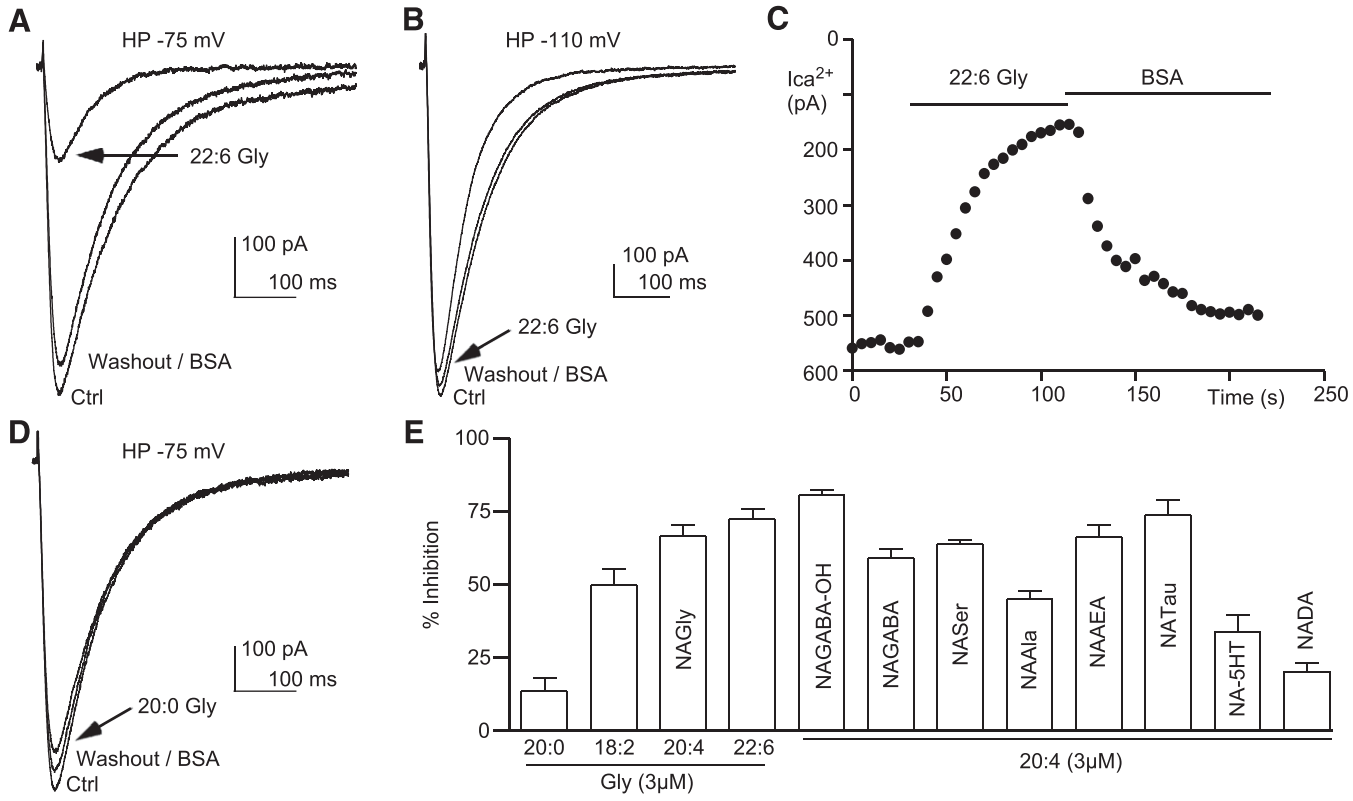

Fig. 1. Inhibition of $Ca_v3.3$ currents by endogenous lipids. (A and B) Inhibition of $Ca_v3.3$ currents by 3 μM 22:6 Gly and subsequent washout with a solution containing 3 mg/ml bovine serum albumin (BSA). $Ca_v3.3$ currents were elicited by a 450-millisecond depolarization to −30 mV from a HP of −75 mV (A) or −110 mV (B) at a frequency of 0.2 Hz. (C) Time course of the decrease in $Ca_v3.3$ current amplitude during 22:6 Gly application at HP −75 mV and subsequent washout with the BSA solution. Same cell as in A. (D) Inhibition of $Ca_v3.3$ currents by 20:0 Gly at HP −75 mV and subsequent washout with a solution containing 3 mg/ml BSA. (E) Summary of the inhibitory effect on $Ca_v3.3$ current at HP −75 mV of 20:0 Gly, 18:2 Gly, *N*AGly, 22:6 Gly, *N*AGABA-OH, *N*AGABA, *N*ASer, *N*AAla, *N*AEA, *N*ATau, *N*A-5HT, and *N*ADA. Ctrl, control.

(18:2 Gly) produced ~50% inhibition ($n = 7$; Fig. 1E; $P \leq 0.001$ compared with 20:0 Gly); *N*-arachidonoyl glycine (20:4, *N*AGly) produced ~67% inhibition ($n = 11$; Fig. 1E; $P \leq 0.05$ compared with 18:2 Gly); and the fully polyunsaturated 22:6 glycine produced ~74% inhibition ($n = 12$; Fig. 1E; not statistically significant compared with 20:4 Gly). Interestingly, the increase in the number of double bonds in fatty acids augmented the membrane fluidity while restricting the conformational freedom of the molecule, possibly leading to the adequate conformation to inhibit the T-current.

The $Ca_v3.3$ current was also inhibited by several *N*-arachidonoyl amino acids, including *N*-arachidonoyl-3-OH-γ-butyric acid (*N*AGABA-OH, ~81% inhibition, $n = 22$), *N*-arachidonoyl-γ-butyric acid (*N*AGABA, ~59% inhibition, $n = 24$), *N*-arachidonoyl-L-serine (*N*ASer, ~64% inhibition, $n = 22$), and *N*-arachidonoyl alanine (*N*AAla, ~45% inhibition, $n = 23$; Fig. 1E). In addition, the lipo-neurotransmitters *N*-arachidonoyl taurine (*N*ATau), *N*A-5HT, and *N*-arachidonoyl dopamine (*N*ADA) inhibited the $Ca_v3.3$ current by ~74%, ~34%, and ~20%, respectively ($n \geq 8$; Fig. 1E). Similar findings were obtained with *N*ADA and *N*A-5HT using an intracellular medium containing 10 mM BAPTA ($n = 5$) (Ross et al., 2009; Gilmore et al., 2012) as well as on $Ca_v3.1$ and $Ca_v3.2$ current (data not shown). Application of 3 μM *N*ADA induced ~18% inhibition of the $Ca_v3.1$ current ($n = 5$) and ~27% inhibition of the $Ca_v3.2$ current ($n = 6$). Similarly, application of 3 μM *N*A-5HT induced ~44% inhibition of the $Ca_v3.1$ current ($n = 16$) and ~50% inhibition of the $Ca_v3.2$ current ($n = 14$). As previously described elsewhere (Chemin et al., 2001), in these experiments, 3 μM *N*AEA [*N*-arachidonoyl ethanolamine (anandamide)] strongly inhibited the three Ca_v3 currents by ~74%–80% ($n \geq 8$; Fig. 1E).

***N*AGly Effect on $Ca_v3.3$ Biophysical Properties.** *N*AGly inhibited the $Ca_v3.3$ current at every potential, with inhibition of the peak current at −35 mV by ~40% with 1 μM *N*AGly and by ~70% with 3 μM *N*AGly (Fig. 2A). *N*AGly had a weak and not statistically significant effect on the $Ca_v3.3$ current–voltage relationship, as the $V_{0.5}$ values were −45.7 ± 1.3 mV ($n = 8$) in control conditions, −49.6 ± 1.4 mV ($n = 8$) during 1 μM *N*AGly application, and −48.6 ± 0.8 mV ($n = 5$) during 3 μM *N*AGly application ($P > 0.05$). We also observed that 3 μM *N*AGly accelerated the inactivation rate of the $Ca_v3.3$ current at every tested potential ($P < 0.05$, $n = 5$; Fig. 2B) without a significant corresponding effect on the activation rate (Fig. 2C). Furthermore, *N*AGly induced a ~10 mV negative shift in the steady-state inactivation properties of $Ca_v3.3$ (Fig. 2D). The $V_{0.5}$ values were −73.1 ± 0.9 mV ($n = 8$) in control conditions, −80.6 ± 1.07 mV ($P < 0.001$, $n = 8$) during 1 μM *N*AGly application, and −83.2 ± 0.8 mV ($P < 0.001$, $n = 7$) during 3 μM *N*AGly application. Application of 3 μM *N*AGly also decreased the slope factor of the steady-state inactivation curve of $Ca_v3.3$ from 5.2 ± 0.2 in control conditions to 4.3 ± 0.2 ($P < 0.05$).

We next investigated the effect of *N*AGly on the recovery from inactivation of the $Ca_v3.3$ current (Fig. 2E). The recovery from inactivation of the $Ca_v3.3$ current was well

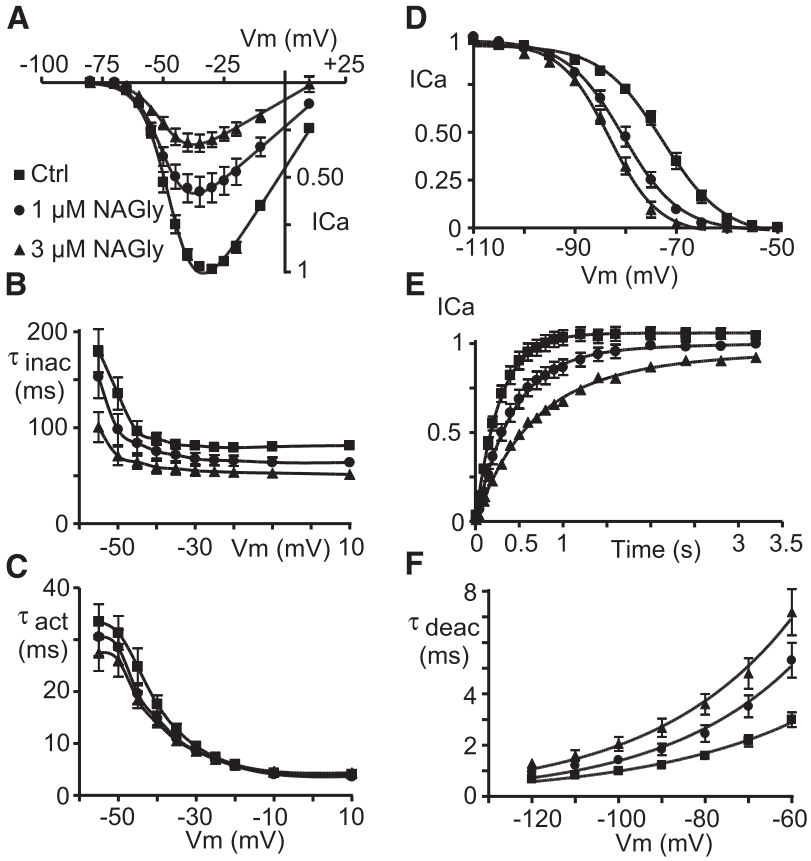

Fig. 2. Effects of *N*AGly on biophysical properties of $Ca_v3.3$ currents. (A) Current-voltage (I-V) curves of $Ca_v3.3$ current in the absence or presence of 1 or 3 μM *N*AGly. Currents were elicited by increasing depolarizations (−80 to +10 mV) from a HP of −80 mV at a frequency of 0.2 Hz. (B–C) Effects of 1 and 3 μM *N*AGly on inactivation (τ_{inac}; B) and activation (τ_{act}; C) kinetics of $Ca_v3.3$ currents. (D) Steady-state inactivation curves of $Ca_v3.3$ currents in the absence or presence of 1 or 3 μM *N*AGly. Currents were recorded at −30 mV from HPs ranging from −110 to −50 mV (5-second duration). (E) Recovery from inactivation of $Ca_v3.3$ current in the absence or presence of 1 or 3 μM *N*AGly. Recovery from inactivation was measured using two −30 mV depolarizations lasting 450 milliseconds, which were applied from a HP of −80 mV of increasing duration. (F) Effects of 1 or 3 μM *N*AGly on deactivation kinetics of $Ca_v3.3$ currents (τ_{deac}). Currents were elicited by a 28-millisecond depolarization at −30 mV, and deactivation kinetics were measured at repolarization potentials ranging from −130 to −60 mV. Ctrl, control.

fit by a monoexponential revealing that *N*AGly strongly increased the τ of recovery from 298 ± 20 milliseconds ($n = 8$) in control conditions to 453 ± 22 milliseconds ($P < 0.001$, $n = 8$) during 1 μM *N*AGly application and to 771 ± 43 milliseconds ($P < 0.001$, $n = 8$) during 3 μM *N*AGly application. Finally, we found that both 1 and 3 μM *N*AGly slowed the deactivation of the $Ca_v3.3$ current at repolarization potentials ranging from −120 to −60 mV ($P < 0.05$, $n = 8$; Fig. 2F).

Pharmacologic Interaction of Endogenous Lipids and TTA-A2 on the $Ca_v3.3$ Channel. Recently, TTA-A2, a potent and specific synthetic inhibitor of T-current, was described (Uebele et al., 2009a,b; Kraus et al., 2010; Reger et al., 2011). As observed with endogenous lipids, TTA-A2 inhibited the Ca_v3 current at physiologic HP but not at very negative potentials (i.e., −110 mV) (Kraus et al., 2010; Francois et al., 2013). Furthermore, as observed with endogenous lipids, TTA-A2 induced a negative shift in the steady-state inactivation properties of Ca_v3 current and slowed their recovery from inactivation (Kraus et al., 2010; Francois et al., 2013). It should be noted that several other structurally unrelated T-channel inhibitors, including mibefradil, flunarizine, and pimozide, which also exhibit similar state-dependent inhibition of T-currents (Martin et al., 2000; Santi et al., 2002), were shown to interact with [^{3}H]TTA-A1 binding to membranes containing $Ca_v3.3$ (Uebele et al., 2009b).

Therefore, we investigated whether endogenous lipids and TTA-A2 could share a common inhibitory mechanism on $Ca_v3.3$. To this purpose, the effect of *N*AEA (which strongly inhibited $Ca_v3.3$ current) and *N*ADA or *N*A-5HT (which mildly inhibited $Ca_v3.3$ current) were compared in the presence and the absence of TTA-A2 (Fig. 3). We found that 300 nM *N*AEA alone induced 56% ± 2% inhibition of the $Ca_v3.3$ current and accelerated the inactivation kinetic (τ) by 32.5% ± 2.6% ($P < 0.05$, $n = 8$; Fig. 3A), as previously described elsewhere (Chemin et al., 2001). Similarly, 3 nM TTA-A2 alone induced 52% ± 3% inhibition of the $Ca_v3.3$ current but slowed the inactivation kinetic (τ) by 34.1% ± 5.4% ($P < 0.05$, $n = 7$; Fig. 3B).

Interestingly, when *N*AEA and TTA-A2 were applied simultaneously, the $Ca_v3.3$ current was inhibited by 70% ± 2% ($n = 10$; Fig. 3C), indicating that the effect of *N*AEA and TTA-A2 are only partially additive (Fig. 3G). In this latter case, the inactivation kinetic (τ) was accelerated by 21.7% ± 4.9% ($P < 0.05$, $n = 10$; Fig. 3C). The results were not different ($P > 0.05$) when both molecules were applied after *N*AEA application ($n = 5$; Fig. 3A) or TTA-A2 application ($n = 5$; Fig. 3B).

These results were further confirmed using the mild inhibitors *N*ADA and *N*A-5HT. Indeed, when 3 μM *N*A-5HT, which inhibited the $Ca_v3.3$ current by 20% ± 4% ($n = 16$; Fig. 3D), was applied with TTA-A2, the resulting inhibition was only 33% ± 4% ($n = 19$; Fig. 3F), demonstrating no additive effects. This was clearly evidenced when *N*A-5HT and TTA-A2 were applied together after TTA-A2 treatment (Fig. 3E). In this case, the inhibition induced by both compounds was less than those obtained with TTA-A2 alone ($P < 0.01$, $n = 11$; Fig. 3, E and G). Similar findings were obtained with 3 μM *N*ADA ($n = 15$; Fig. 3G).

Overall, these results demonstrated a pharmacologic interaction between endogenous lipids and TTA-A2 and suggested that both molecules could share the same molecular site on the $Ca_v3.3$ protein.

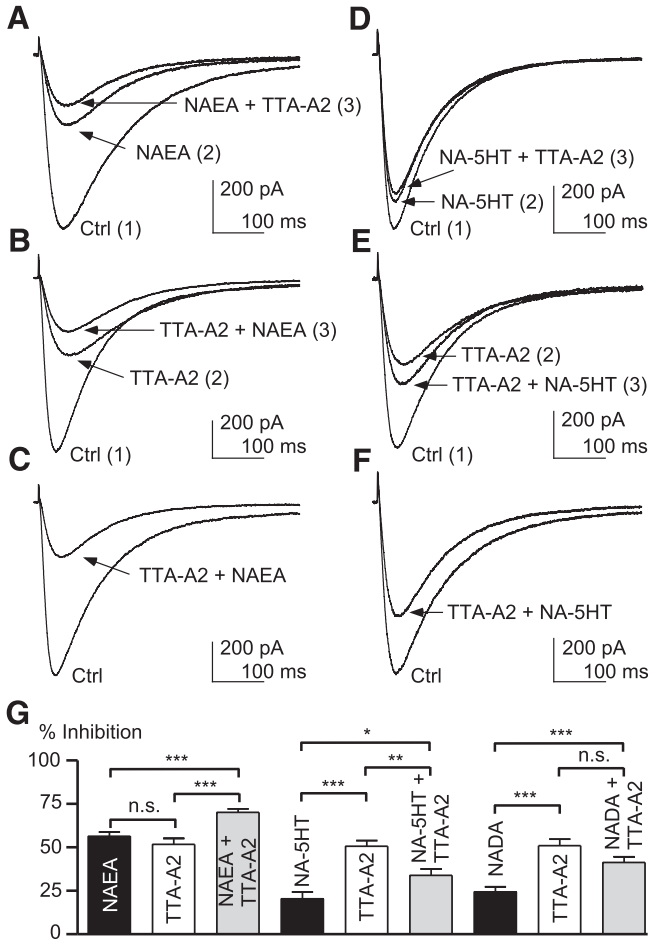

Fig. 3. Inhibition of $Ca_v3.3$ currents by combined application of endogenous lipids and TTA-A2. (A) Effect of a 300 nM *N*AEA solution (2) followed by the application of both 300 nM *N*AEA and 3 nM TTA-A2 (3), compared with the control solution (1). (B) Effect of a 3 nM TTA-A2 solution followed by the application of both 300 nM *N*AEA and 3 nM TTA-A2. (C) Effect of a solution containing both 300 nM *N*AEA and 3 nM TTA-A2. (D–F) Similar experiments with 3 μM *N*A-5HT and 3 nM TTA-A2. (G) Summary of the average effects of *N*AEA, *N*ADA, and *N*A-5HT alone or combined with 3 nM TTA-A2. Currents were elicited at −30 mV from a HP of −75 mV at a frequency of 0.2 Hz. $^*P < 0.05$; $^{**}P < 0.01$; $^{***}P < 0.001$. Ctrl, control; n.s., not statistically significant.

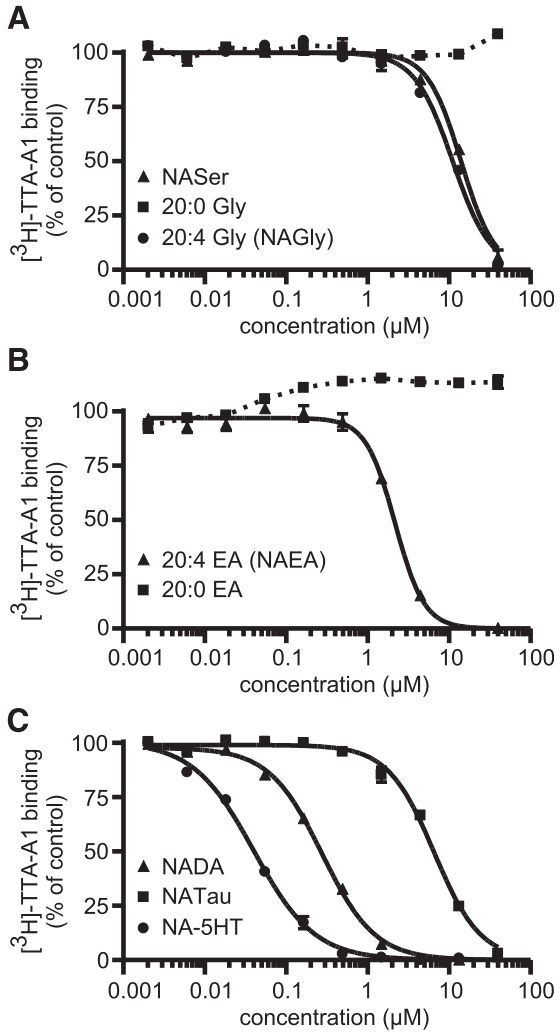

Fig. 4. Displacement of [^{3}H]TTA-A1 binding by (A) *N*-acyl amino acids, (B) *N*-acyl ethanolamines, and (C) *N*-acyl neurotransmitters. Lipids are *N*ASer, *N*AGly, 20:0 Gly, *N*AEA (20:4), *N*-arachidoyl ethanolamine (20:0 EA), *N*ADA (20:4), *N*A-5HT (20:4), and *N*ATau (20:4).

***N*-Acyl Derivatives That Inhibited $Ca_v3.3$ Current Displaced [^{3}H]TTA-A1 Binding.** Because lipids and TTA-A2 possibly act at the same molecular site, we investigated whether bioactive lipids that inhibit $Ca_v3.3$ current could displace [^{3}H]TTA-A1 (a radiolabeled derivative of TTA-A2) binding to membranes containing $Ca_v3.3$, as demonstrated for several state-dependent T-channel antagonists (Uebele et al., 2009b). We found that *N*-arachidonoyl amino-acids *N*ASer and *N*AGly, which inhibited $Ca_v3.3$ current (Fig. 1D), displaced [^{3}H]TTA-A1 binding in a concentration-dependent manner (Fig. 4A). The K_i for *N*ASer was 9.02 ± 0.06 μM and 7.12 ± 0.31 μM for *N*AGly whereas the Hill slope number (n_{Hill}) was 2.1 and 1.8 for *N*ASer and *N*AGly, respectively.

Displacement of [^{3}H]TTA-A1 binding was not observed with the saturated arachidoyl glycine at concentrations up to 40 μM (20:0; Fig. 4A). Similarly, the endocannabinoid anandamide (20:4 EA) displaced [^{3}H]TTA-A1 binding with a K_i of 1.35 ± 0.04 μM and a n_{Hill} of 2.4, but not the saturated form, *N*-arachidoyl ethanolamine (Fig. 4B). In addition, the *N*-arachidonoyl neurotransmitters *N*ATau, *N*-arachidonoyl dopamine (*N*ADA) and *N*A-5HT, also displaced [^{3}H]TTA-A1 binding (Fig. 4C). The K_i was 4.13 ± 0.11 μM for *N*ATau, 0.170 ± 0.004 μM for *N*ADA and 0.026 ± 0.001 μM for *N*A-5HT whereas the n_{Hill} was 1.5, 1.3, and 1.1 for *N*ATau, *N*ADA, and *N*A-5HT, respectively.

TTA-Q4, a Positive Allosteric Modulator of [^{3}H]TTA-A1 Binding, Increased Lipid-Induced Inhibition of $Ca_v3.3$ Current. The structurally distinct T-type antagonist TTA-Q4 was shown to increase [^{3}H]TTA-A1 binding on $Ca_v3.3$ expressing membranes as well as TTA-A2–induced $Ca_v3.3$ current inhibition (Uebele et al., 2009b). It was demonstrated that TTA-Q4 increased TTA-A2–mediated $Ca_v3.3$ current inhibition by a synergistic mechanism (Uebele et al., 2009b). Therefore, we investigated whether TTA-Q4 had a similar effect on lipid-induced $Ca_v3.3$ current inhibition.

We found that 20 nM TTA-Q4 alone induced 22% ± 4% inhibition of $Ca_v3.3$ current (n = 8; Fig. 5A), 100 nM anandamide alone induced 18% ± 5% inhibition (n = 5; Fig. 5B), but application of both compounds induced 72% ± 4% inhibition (n = 7; Fig. 5, C and D), which is much greater than

the anticipated sum of ~40% expected for additive effects (as indicated by an arrow in Fig. 5I). We also found that 300 nM *N*A-5HT induced a negligible effect on $Ca_v3.3$ current (8% ± 5% inhibition, $n = 5$; Fig. 5E) whereas when *N*A-5HT was applied with TTA-Q4, the inhibition of $Ca_v3.3$ current was 52% ± 2% ($n = 5$; Fig. 5, G–I). Similar results were obtained using 3 μM *N*ADA and 20 nM TTA-Q4, as application of both compounds induced 72% ± 2% inhibition of $Ca_v3.3$ current ($n = 11$; Fig. 5I). Overall, these results indicated that TTA-Q4 and polyunsaturated lipids modulated $Ca_v3.3$ current in a synergistic manner.

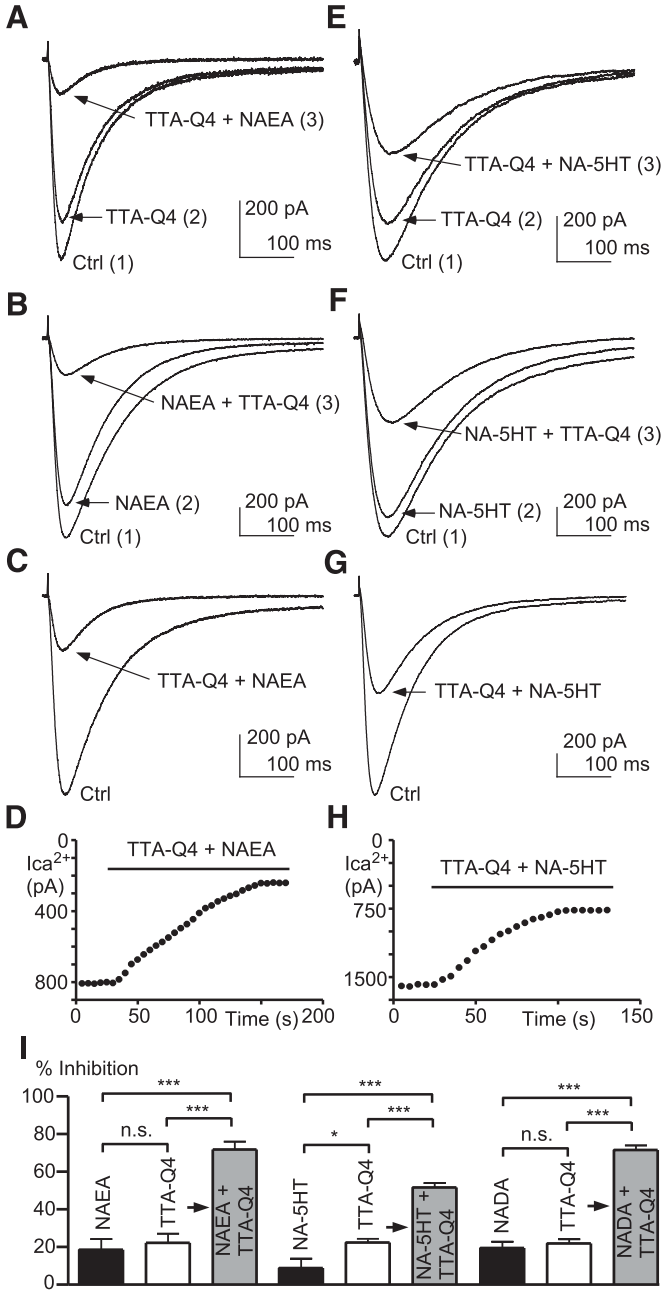

Fig. 5. Inhibition of $Ca_v3.3$ currents by combined application of endogenous lipids and TTA-Q4. (A) Effect of a 20 nM TTA-Q4 solution followed by the application of both 100 nM *N*AEA and 20 nM TTA-Q4. (B) Effect of a 100 nM *N*AEA solution followed by the application of both 100 nM *N*AEA and 20 nM TTA-Q4. (C) Effect of a solution containing both 100 nM *N*AEA and 20 nM TTA-Q4. (D) Time course of the decrease in $Ca_v3.3$ current amplitude during application of 100 nM *N*AEA and 20 nM TTA-Q4. Same cell as in C. (E–H) Similar experiments with 20 nM TTA-Q4 and 300 nM *N*A-5HT. (I) Summary of the effects of *N*AEA, *N*ADA, and *N*A-5HT alone or combined with 20 nM TTA-Q4. The arrows indicate the anticipated sum of the effects of lipids plus TTA-Q4. Currents were elicited at −30 mV from a HP of −75 mV at a frequency of 0.2 Hz. $^*P < 0.05$; $^{***}P < 0.001$. Ctrl, control; n.s., not statistically significant.

Discussion

In this study, we demonstrated that lipid effects on $Ca_v3.3$ biophysical properties share many features with those induced by TTA-A2, especially regarding the gating properties. Importantly, inhibition of $Ca_v3.3$ current by both lipids and TTA-A2 occurs only at depolarized resting potentials at which $Ca_v3.3$ channels are partly inactivated. We also documented that endogenous lipids and TTA-A2 share similar molecular mechanisms.

First, we found that TTA-A2 effects on $Ca_v3.3$ current were weakly additive with those produced by lipids or were even decreased when both lipids and TTA-A2 were applied together. Second, using [^{3}H]TTA-A1, a radioactive derivative of TTA-A2 that specifically binds membranes expressing $Ca_v3.3$ (Uebele et al., 2009b), we found that endogenous lipids inhibiting $Ca_v3.3$ all displaced [^{3}H]TTA-A1 binding, with K_i in the micromolar range. Third, using TTA-Q4, which increased [^{3}H]TTA-A1 binding on $Ca_v3.3$ expressing membranes as well as TTA-A2–induced $Ca_v3.3$ current inhibition (Uebele et al., 2009b), we demonstrated a synergistic mechanism between this molecule and lipids for $Ca_v3.3$ current inhibition.

Overall, our results indicate a common molecular mechanism between the synthetic inhibitor TTA-A2 and the endogenous lipids, and suggest that lipids inhibiting the T-current could act directly on the $Ca_v3.3$ protein at a site overlapping that of TTA-A2. However, we cannot exclude that lipids could displace [^{3}H]TTA-A1 binding by acting at the membrane rather than on the $Ca_v3.3$ protein. Importantly, no [^{3}H]TTA-A1 binding was observed in membranes from HEK-293 cells that did not express $Ca_v3.3$ (Uebele et al., 2009b).

We have shown that *N*-arachidonoyl derivatives containing a glycine, a serine, an alanine, a γ-butyric acid, a 3-OH-γ-butyric acid, and a taurine inhibited the $Ca_v3.3$ current. Inhibition did not occur with the saturated *N*-arachidoyl glycine (20:0 Gly) and increased with the number of double bonds, leading to maximal effect on $Ca_v3.3$ current with the fully polyunsaturated ω3 22:6 Gly. Similar findings were obtained for $Ca_v3.1$ and $Ca_v3.2$ currents (not shown), as previously observed with fatty acids and *N*-acyl ethanolamines (Chemin et al., 2007).

In contrast with previous studies (Ross et al., 2009; Gilmore et al., 2012), we found that *N*A-5HT and *N*ADA were weak inhibitors of the $Ca_v3.3$ currents (as well as $Ca_v3.1$ and $Ca_v3.2$ currents). Similar results were obtained using a stable HEK-293 cell line expressing $Ca_v3.3$ current or using an intracellular medium containing 10 mM BAPTA (Ross et al., 2009; Gilmore et al., 2012). We do not have yet any satisfactory explanation for this discrepancy because the Ca_v3 subunits and the lipids used here are identical and from the same companies as those previously used (Ross et al., 2009; Gilmore et al., 2012).

We also demonstrated that the inhibition occurred only at depolarized resting potentials, indicating that lipids preferentially affect T-channels in the inactivated state or in intermediate

closed states (Talavera et al., 2004). Furthermore, *N*AGly induced a hyperpolarized shift in the $Ca_v3.3$ steady-state inactivation properties, leading to current inhibition at physiologic resting potentials. In addition, we found that *N*AGly slowed the recovery from inactivation of the $Ca_v3.3$ current, a property that was not investigated before on recombinant channels. These effects on inactivation properties were reminiscent of those induced by TTA-A2, which induced similar effects on steady-state inactivation and recovery from inactivation (Kraus et al., 2010; Francois et al., 2013).

*N*AGly also induced a hyperpolarized shift in the steady-state inactivation of $Ca_v3.1$ and $Ca_v3.2$ currents and slowed their recovery from inactivation confirming a common biophysical mechanism (data not shown). However, *N*AGly had specific effects on the $Ca_v3.3$ current kinetics. *N*AGly accelerated the inactivation kinetics of $Ca_v3.3$ current at every tested potential without the corresponding effect on $Ca_v3.1$ and $Ca_v3.2$ currents (data not shown). In the same way, *N*AGly induced a deceleration of the $Ca_v3.3$ deactivation kinetic, which was not observed on $Ca_v3.1$ or $Ca_v3.2$ currents (data not shown) and is not yet documented for TTA-A2.

We found that TTA-A2–induced inhibition of $Ca_v3.3$ current was not fully additive with those produced by anandamide when both compounds were applied together. Moreover, the presence of *N*ADA or *N*A-5HT decreased the TTA-A2 effect, probably because they did not produce an important inhibition per se, which suggests that they could share with TTA-A2 a common site on $Ca_v3.3$. This was confirmed using [^{3}H]TTA-A1, a radioactive derivative of TTA-A2 that specifically binds membranes expressing $Ca_v3.3$ (Uebele et al., 2009b). Indeed, we demonstrated that polyunsaturated lipids *N*AGly, *N*ASer, *N*AEA, *N*ADA, *N*A-5HT, and *N*ATau all displaced the [^{3}H]TTA-A1 binding, with K_i in a micromolar or submicromolar range whereas saturated lipids (which did not inhibit $Ca_v3.3$ current) had no effect. The affinity (K_i in μM) obtained with polyunsaturated lipids was *N*A-5HT (0.02) < *N*ADA (0.17) < *N*AEA (1.35) < *N*ATau (4.13) < *N*AGly (7.12) < *N*ASer (9.02). These findings are in good agreement with our electrophysiologic studies on $Ca_v3.3$ current inhibition.

Interestingly, we also found that *N*ADA and *N*A-5HT, which had a mild effect on $Ca_v3.3$ current, strongly bound to $Ca_v3.3$-expressing membranes. Accordingly, the presence of *N*ADA or *N*A-5HT prevented TTA-A2 inhibitory effects in electrophysiologic experiments. We had previously shown that the inhibitory effects of lipids on the T-current depend on both the amide and the hydroxyl groups (Chemin et al., 2007). In this context, the aromatic heterocyclic rings of *N*ADA and *N*A-5HT, which increase the distance between the amide and the hydroxyl groups and are also hydrophobic, could impair interaction with key amino acids in the $Ca_v3.3$ protein and therefore their inhibitory effect without decreasing their binding to membranes expressing $Ca_v3.3$. This suggests that the polyunsaturated alkyl chain of lipids would be mostly important for their binding whereas the amide and hydroxyl groups would mediate current inhibition. Accordingly, both *N*ADA and *N*A-5HT strongly occluded the TTA-A2 effect but weakly inhibited the $Ca_v3.3$ current whereas saturated lipids (which did not produce inhibition) provided no consistent displacement.

We also found that the Hill slope number (n_{Hill}) in these binding assays was high (ranging from 1.5 to 2.4) for *N*ATau, *N*AGly, *N*ASer, and *N*AEA, especially for *N*AEA (n_{Hill} = 2.4), whereas the n_{Hill} for *N*A-5HT and *N*ADA was more typical of competitive displacement curves (n_{Hill} between 1.1 and 1.3). These results might indicate lipid degradation, because in these binding experiments we did not use a fatty acid amide hydrolase [FAAH, the main enzyme metabolizing *N*AEA and others *N*Arachidonoyl-conjugates (Huang et al., 2001; Saghatelian et al., 2004, 2006)] inhibitor and this enzyme is known to be very active even in crude membrane extracts (Deutsch and Chin, 1993; Childers et al., 1994; Pinto et al., 1994). For instance, displacement of the cannabinoid receptor 1 agonist [^{3}H]CP-55940 (1*R*,3*R*,4*R*)-3-[2-hydroxy-4-(1,1-dimethylheptyl)phenyl]-4-(3-hydroxypropyl)cyclohexan-1-ol) by *N*AEA indicated a K_i of 2 μM in the absence of the FAAH inhibitor phenylmethylsulfonyl fluoride (PMSF) whereas the K_i was 12 nM in the presence of PMSF (Pinto et al., 1994), suggesting *N*AEA degradation. Interestingly, the same investigators showed that the slope of the displacement curve was particularly steep ($n_{Hill} > 2$) in the absence of PMSF whereas in the presence of PMSF the n_{Hill} was near a value of 1 (Pinto et al., 1994). It is also interesting that *N*A-5HT and *N*ADA are inhibitors of FAAH and particularly *N*A-5HT (Bisogno et al., 1998, 2000) and this FAAH inhibition could account for the strong *N*A-5HT potency in the binding assay. Moreover, it is important to note that in these membrane extracts the transmembrane resting potential was likely lost, and the $Ca_v3.3$ channels might be in a complete inactivated state that was not achieved in electrophysiologic experiments, which could also explain the potency of *N*A-5HT and *N*ADA in these binding assays.

Because the structurally distinct antagonist TTA-Q4 was shown to be a positive allosteric modulator of TTA-A2, increasing [^{3}H]TTA-A1 binding on $Ca_v3.3$-expressing membranes as well as TTA-A2 induced $Ca_v3.3$ current inhibition (Uebele et al., 2009b), we have investigated whether it could also promote lipid-induced $Ca_v3.3$ current inhibition. We found that TTA-Q4 potentiated the *N*AEA effect on $Ca_v3.3$ current, indicating that TTA-Q4 and anandamide could inhibit $Ca_v3.3$ current in a synergistic manner. Moreover, in the presence of TTA-Q4 we revealed important *N*ADA and *N*A-5HT inhibitory effects, as previously described elsewhere (Ross et al., 2009; Gilmore et al., 2012). Interestingly, the binding and the potency of anandamide at cannabinoid receptor 1 and transient receptor potential vanilloid-1 receptors is increased by palmitoyl ethanolamine and oleoyl ethanolamine, which act as an allosteric modulator of these receptors in a phenomenon called the "entourage" effect (Ben-Shabat et al., 1998; De Petrocellis et al., 2001; Ho et al., 2008).

It has been demonstrated that TTA-A2 has important pharmacologic effects, including the reduction of absence epilepsy seizures (Uebele et al., 2009b; Reger et al., 2011) and of pain perception (Francois et al., 2013). In addition, TTA-A2 affects sleep/wake patterns (Uebele et al., 2009a; Kraus et al., 2010; Reger et al., 2011) and displays antipsychotic properties (Uslaner et al., 2012). Similarly, bioactive lipids inhibiting T-currents have been implicated in several functions, including pain perception (Bradshaw and Walker, 2005; Burstein, 2008; Basbaum et al., 2009), sleep, and epilepsy (Chen and Bazan, 2005). The analogy between in vivo effects of TTA-A2 and lipids suggests, in the light of our results, that many physiologic effects of endogenous lipids are supported by T-current inhibition. Furthermore, TTA-A2 and TTA-Q4 could be important

pharmacologic tools to dissect the involvement of T-current in the physiologic effects of endogenous lipids.

Acknowledgments

The authors thank Drs. T. Durroux and F. Rassendren for insightful discussions and critical reading of the manuscript.

Authorship Contributions

Participated in research design: Uebele, Lory, Chemin.

Conducted experiments: Cazade, Nuss, Bidaud, Chemin.

Contributed new reagents or analytic tools: Renger, Uebele.

Performed data analysis: Uebele, Chemin.

Wrote or contributed to the writing of the manuscript: Uebele, Lory, Chemin.

References

Barbara G, Alloui A, Nargeot J, Lory P, Eschalier A, Bourinet E, and Chemin J (2009) T-type calcium channel inhibition underlies the analgesic effects of the endogenous lipoamino acids. *J Neurosci* **29**:13106–13114.

Basbaum AI, Bautista DM, Scherrer G, and Julius D (2009) Cellular and molecular mechanisms of pain. *Cell* **139**:267–284.

Ben-Shabat S, Fride E, Sheskin T, Tamiri T, Rhee MH, Vogel Z, Bisogno T, De Petrocellis L, Di Marzo V, and Mechoulam R (1998) An entourage effect: inactive endogenous fatty acid glycerol esters enhance 2-arachidonoyl-glycerol cannabinoid activity. *Eur J Pharmacol* **353**:23–31.

Bisogno T, Melck D, Bobrov MYu, Gretskaya NM, Bezuglov VV, De Petrocellis L, and Di Marzo V (2000) N-acyl-dopamines: novel synthetic CB(1) cannabinoid-receptor ligands and inhibitors of anandamide inactivation with cannabimimetic activity in vitro and in vivo. *Biochem J* **351**:817–824.

Bisogno T, Melck D, De Petrocellis L, Bobrov MYu, Gretskaya NM, Bezuglov VV, Sitachitta N, Gerwick WH, and Di Marzo V (1998) Arachidonoylserotonin and other novel inhibitors of fatty acid amide hydrolase. *Biochem Biophys Res Commun* **248**:515–522.

Bradshaw HB and Walker JM (2005) The expanding field of cannabimimetic and related lipid mediators. *Br J Pharmacol* **144**:459–465.

Burstein S (2008) The elmiric acids: biologically active anandamide analogs. *Neuropharmacology* **55**:1259–1264.

Cain SM and Snutch TP (2010) Contributions of T-type calcium channel isoforms to neuronal firing. *Channels (Austin)* **4**:475–482.

Chemin J, Monteil A, Perez-Reyes E, Nargeot J, and Lory P (2001) Direct inhibition of T-type calcium channels by the endogenous cannabinoid anandamide. *EMBO J* **20**:7033–7040.

Chemin J, Nargeot J, and Lory P (2007) Chemical determinants involved in anandamide-induced inhibition of T-type calcium channels. *J Biol Chem* **282**: 2314–2323.

Chen C and Bazan NG (2005) Lipid signaling: sleep, synaptic plasticity, and neuroprotection. *Prostaglandins Other Lipid Mediat* **77**:65–76.

Childers SR, Sexton T, and Roy MB (1994) Effects of anandamide on cannabinoid receptors in rat brain membranes. *Biochem Pharmacol* **47**:711–715.

Danthi SJ, Enyeart JA, and Enyeart JJ (2005) Modulation of native T-type calcium channels by omega-3 fatty acids. *Biochem Biophys Res Commun* **327**:485–493.

De Petrocellis L, Davis JB, and Di Marzo V (2001) Palmitoylethanolamide enhances anandamide stimulation of human vanilloid VR1 receptors. *FEBS Lett* **506**: 253–256.

Deutsch DG and Chin SA (1993) Enzymatic synthesis and degradation of anandamide, a cannabinoid receptor agonist. *Biochem Pharmacol* **46**:791–796.

Francois A, Kerckhove N, Meleine M, Alloui A, Barrere C, Gelot A, Uebele VN, Renger JJ, Eschalier A, and Ardid D et al. (2013) State-dependent properties of a new T-type calcium channel blocker enhance Ca(V)3.2 selectivity and support analgesic effects. *Pain* **154**:283–293.

Gilmore AJ, Heblinski M, Reynolds A, Kassiou M, and Connor M (2012) Inhibition of human recombinant T-type calcium channels by N-arachidonoyl 5-HT. *Br J Pharmacol* **167**:1076–1088.

Giordanetto F, Knerr L, and Wållberg A (2011) T-type calcium channels inhibitors: a patent review. *Expert Opin Ther Pat* **21**:85–101.

Ho WS, Barrett DA, and Randall MD (2008) 'Entourage' effects of N-palmitoylethanolamide and N-oleoylethanolamide on vasorelaxation to anandamide occur through TRPV1 receptors. *Br J Pharmacol* **155**:837–846.

Huang SM, Bisogno T, Petros TJ, Chang SY, Zavitsanos PA, Zipkin RE, Sivakumar R, Coop A, Maeda DY, and De Petrocellis L et al. (2001) Identification of a new class of molecules, the arachidonyl amino acids, and characterization of one member that inhibits pain. *J Biol Chem* **276**:42639–42644.

Kraus RL, Li Y, Gregan Y, Gotter AL, Uebele VN, Fox SV, Doran SM, Barrow JC, Yang ZQ, and Reger TS et al. (2010) In vitro characterization of T-type calcium channel antagonist TTA-A2 and in vivo effects on arousal in mice. *J Pharmacol Exp Ther* **335**:409–417.

Kuo IY, Wölfle SE, and Hill CE (2011) T-type calcium channels and vascular function: the new kid on the block? *J Physiol* **589**:783–795.

Leaf A, Xiao YF, Kang JX, and Billman GE (2003) Prevention of sudden cardiac death by n-3 polyunsaturated fatty acids. *Pharmacol Ther* **98**:355–377.

Lee J and Shin HS (2007) T-type calcium channels and thalamocortical rhythms in sleep: a perspective from studies of T-type calcium channel knockout mice. *CNS Neurol Disord Drug Targets* **6**:63–69.

Lory P, Bidaud I, and Chemin J (2006) T-type calcium channels in differentiation and proliferation. *Cell Calcium* **40**:135–146.

Lory P and Chemin J (2007) Towards the discovery of novel T-type calcium channel blockers. *Expert Opin Ther Targets* **11**:717–722.

Martin RL, Lee JH, Cribbs LL, Perez-Reyes E, and Hanck DA (2000) Mibefradil block of cloned T-type calcium channels. *J Pharmacol Exp Ther* **295**:302–308.

McGivern JG (2006) Pharmacology and drug discovery for T-type calcium channels. *CNS Neurol Disord Drug Targets* **5**:587–603.

Ono K and Iijima T (2010) Cardiac T-type $Ca^{(2+)}$ channels in the heart. *J Mol Cell Cardiol* **48**:65–70.

Perez-Reyes E (2003) Molecular physiology of low-voltage-activated t-type calcium channels. *Physiol Rev* **83**:117–161.

Pinto JC, Potié F, Rice KC, Boring D, Johnson MR, Evans DM, Wilken GH, Cantrell CH, and Howlett AC (1994) Cannabinoid receptor binding and agonist activity of amides and esters of arachidonic acid. *Mol Pharmacol* **46**:516–522.

Reger TS, Yang ZQ, Schlegel KA, Shu Y, Mattern C, Cube R, Rittle KE, McGaughey GB, Hartman GD, and Tang C et al. (2011) Pyridyl amides as potent inhibitors of T-type calcium channels. *Bioorg Med Chem Lett* **21**:1692–1696.

Roman RJ (2002) P-450 metabolites of arachidonic acid in the control of cardiovascular function. *Physiol Rev* **82**:131–185.

Ross HR, Gilmore AJ, and Connor M (2009) Inhibition of human recombinant T-type calcium channels by the endocannabinoid N-arachidonoyl dopamine. *Br J Pharmacol* **156**:740–750.

Saghatelian A, McKinney MK, Bandell M, Patapoutian A, and Cravatt BF (2006) A FAAH-regulated class of N-acyl taurines that activates TRP ion channels. *Biochemistry* **45**:9007–9015.

Saghatelian A, Trauger SA, Want EJ, Hawkins EG, Siuzdak G, and Cravatt BF (2004) Assignment of endogenous substrates to enzymes by global metabolite profiling. *Biochemistry* **43**:14332–14339.

Santi CM, Cayabyab FS, Sutton KG, McRory JE, Mezeyova J, Hamming KS, Parker D, Stea A, and Snutch TP (2002) Differential inhibition of T-type calcium channels by neuroleptics. *J Neurosci* **22**:396–403.

Talavera K, Staes M, Janssens A, Droogmans G, and Nilius B (2004) Mechanism of arachidonic acid modulation of the T-type Ca^{2+} channel alpha1G. *J Gen Physiol* **124**:225–238.

Todorovic SM and Jevtovic-Todorovic V (2013) Neuropathic pain: role for presynaptic T-type channels in nociceptive signaling. *Pflugers Arch* **465**:921–927.

Uebele VN, Gotter AL, Nuss CE, Kraus RL, Doran SM, Garson SL, Reiss DR, Li Y, Barrow JC, and Reger TS et al. (2009a) Antagonism of T-type calcium channels inhibits high-fat diet-induced weight gain in mice. *J Clin Invest* **119**:1659–1667.

Uebele VN, Nuss CE, Fox SV, Garson SL, Cristescu R, Doran SM, Kraus RL, Santarelli VP, Li Y, and Barrow JC et al. (2009b) Positive allosteric interaction of structurally diverse T-type calcium channel antagonists. *Cell Biochem Biophys* **55**:81–93.

Uslaner JM, Smith SM, Huszar SL, Pachmerhiwala R, Hinchliffe RM, Vardigan JD, Nguyen SJ, Surles NO, Yao L, and Barrow JC et al. (2012) T-type calcium channel antagonism produces antipsychotic-like effects and reduces stimulant-induced glutamate release in the nucleus accumbens of rats. *Neuropharmacology* **62**: 1413–1421.

Uslaner JM, Vardigan JD, Drott JM, Uebele VN, Renger JJ, Lee A, Li Z, Lê AD, and Hutson PH (2010) T-type calcium channel antagonism decreases motivation for nicotine and blocks nicotine- and cue-induced reinstatement for a response previously reinforced with nicotine. *Biol Psychiatry* **68**:712–718.

Weiss N and Zamponi GW (2013) Control of low-threshold exocytosis by T-type calcium channels. *Biochim Biophys Acta* **1828**:1579–1586.

Xie X, Van Deusen AL, Vitko I, Babu DA, Davies LA, Huynh N, Cheng H, Yang N, Barrett PQ, and Perez-Reyes E (2007) Validation of high throughput screening assays against three subtypes of Ca(v)3 T-type channels using molecular and pharmacologic approaches. *Assay Drug Dev Technol* **5**:191–203.

Zhang Y, Cribbs LL, and Satin J (2000) Arachidonic acid modulation of alpha1H, a cloned human T-type calcium channel. *Am J Physiol Heart Circ Physiol* **278**:H184–H193.

Address correspondence to: Jean Chemin, Institut de Génomique Fonctionnelle, Universités Montpellier 1 & 2, Centre National de la Recherche Scientifique (CNRS), Unité Mixte de Recherche (UMR) 5203, INSERM U661, LabEx Ion Channel Science and Therapeutics, 141, Rue de la Cardonille, 34094 Montpellier CEDEX 05, France. E-mail: jean.chemin@igf.cnrs.fr; or Philippe Lory, Institut de Génomique Fonctionnelle, Universités Montpellier 1 & 2, Centre National de la Recherche Scientifique (CNRS), Unité Mixte de Recherche (UMR) 5203, INSERM U661, LabEx Ion Channel Science and Therapeutics, 141, Rue de la Cardonille, 34094 Montpellier CEDEX 05, France. E-mail: philippe.lory@igf.cnrs.fr